MoM-Based Matrix Operators in AToM

Miloslav Čapek
miloslav.capek@antennatoolbox.com

May 24, 2021

Outline

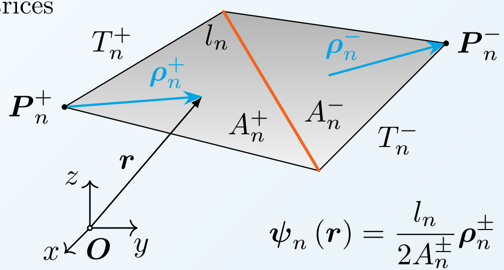

$$\boldsymbol{\psi}_n(\boldsymbol{r}) = \frac{l_n}{2A_n^\pm}\boldsymbol{\rho}_n^\pm$$

Definition of RWG function.

Quadratic form of linear operator $\mathcal{L}$ reads

$$p = \frac{1}{2} \int\limits_{\Omega} \boldsymbol{J}^{*} \cdot \mathcal{L} \left\{ \boldsymbol{J} \right\} \mathrm{d} \boldsymbol{r}, \quad \boldsymbol{J} = \boldsymbol{J} \left(\boldsymbol{r} \right), \boldsymbol{r} \in \Omega. \tag{1}$$

Complex power is defined as

$$P_{\mathrm{rad}} + 2\mathrm{j}\omega \left(W_{\mathrm{m}} - W_{\mathrm{e}} \right) = -\frac{1}{2} \int\limits_{V} \boldsymbol{J}^{*} \cdot \boldsymbol{E} \, \mathrm{d}V \tag{2}$$

Electric Field Integral Equation (EFIE) reads[1]

$$\boldsymbol{E} \left(\boldsymbol{r} \right) = -\mathrm{j} Z_0 k \int\limits_{\Omega} \left(\mathbf{1} + \frac{\nabla \nabla \cdot}{k^2} \right) \boldsymbol{J} \left(\boldsymbol{r}' \right) \frac{\mathrm{e}^{-\mathrm{j} k R}}{4 \pi R} \, \mathrm{d}S, \tag{3}$$

with $\mathbf{1}$ being the identity matrix, $\mathbf{1} = [\delta_{pq}]$.

[1] J. L. Volakis and K. Sertel, *Integral Equation Methods for Electromagnetics*. Scitech Publishing Inc., 2012.

Usage of (finite) discretization of the source region Ω leads to

$$\boldsymbol{J}(\boldsymbol{r}) \approx \sum_{n=1}^{N} I_n \boldsymbol{\psi}_n(\boldsymbol{r}), \tag{4}$$

where $\mathbf{I} = [I_n] \in \mathbb{C}^{N\times 1}$ are expansion coefficients, $\boldsymbol{\psi}_n$ are the basis functions.

Formula (4) transforms (1) into algebraic relation

$$p \approx \frac{1}{2}\mathbf{I}^{\mathrm{H}}\mathbf{L}\mathbf{I} \quad \text{with} \quad L_{mn} \equiv \int\limits_{\Omega} \boldsymbol{\psi}_m \cdot \mathcal{L}\{\boldsymbol{\psi}_n\}\,\mathrm{d}\boldsymbol{r}. \tag{5}$$

Complex power (2) is approximated as

$$P_{\mathrm{rad}} + P_{\mathrm{lost}} + 2\mathrm{j}\omega\,(W_{\mathrm{m}} - W_{\mathrm{e}}) \approx \frac{1}{2}\mathbf{I}^{\mathrm{H}}\mathbf{Z}\mathbf{I}, \tag{6}$$

where $\mathbf{Z} \in \mathbb{C}^{N\times N}$ is the impedance matrix defined as follows.

The vacuum impedance matrix is constructed (from normalized data) as

$$\mathbf{Z}_0 = \mathbf{R}_0 + \mathrm{j}\mathbf{X}_0 = \mathrm{j}Z_0 a^2 \left(ka \left(\mathbf{Z}_0^{\mathrm{m},k} + \mathbf{Z}_0^{\mathrm{m},0} \right) - \frac{1}{ka} \left(\mathbf{Z}_0^{\mathrm{e},k} + \mathbf{Z}_0^{\mathrm{e},0} \right) \right), \tag{7}$$

where individual elements of the defining matrices are

$$Z_{0,mn}^{\mathrm{m},k} = \frac{1}{a^3} \int\limits_{\Omega} \int\limits_{\Omega} \boldsymbol{\psi}_m (\boldsymbol{r}) \cdot \boldsymbol{\psi}_n (\boldsymbol{r}') \, \frac{\mathrm{e}^{-\mathrm{j}kR} - 1}{4\pi R} \, \mathrm{d}S \, \mathrm{d}S', \tag{8}$$

$$Z_{0,mn}^{\mathrm{m},0} = \frac{1}{a^3} \int\limits_{\Omega} \int\limits_{\Omega} \boldsymbol{\psi}_m (\boldsymbol{r}) \cdot \boldsymbol{\psi}_n (\boldsymbol{r}') \, \frac{1}{4\pi R} \, \mathrm{d}S \, \mathrm{d}S', \tag{9}$$

$$Z_{0,mn}^{\mathrm{e},k} = \frac{1}{a} \int\limits_{\Omega} \int\limits_{\Omega} \nabla \cdot \boldsymbol{\psi}_m (\boldsymbol{r}) \, \nabla' \cdot \boldsymbol{\psi}_n (\boldsymbol{r}') \, \frac{\mathrm{e}^{-\mathrm{j}kR} - 1}{4\pi R} \, \mathrm{d}S \, \mathrm{d}S', \tag{10}$$

$$Z_{0,mn}^{\mathrm{e},0} = \frac{1}{a} \int\limits_{\Omega} \int\limits_{\Omega} \nabla \cdot \boldsymbol{\psi}_m (\boldsymbol{r}) \, \nabla' \cdot \boldsymbol{\psi}_n (\boldsymbol{r}') \, \frac{1}{4\pi R} \, \mathrm{d}S \, \mathrm{d}S'. \tag{11}$$

Normalization of characteristic modes[2] to unitary radiated power reads

$$\frac{1}{2} \int\limits_{\Omega} \boldsymbol{J}_p^* \mathcal{Z}_0 \left\{ \boldsymbol{J}_q \right\} \, \mathrm{d}\boldsymbol{r} = \left(1 + \mathrm{j}\lambda_p\right) \delta_{pq}. \tag{12}$$

The same normalization based on impedance matrix is[3]

$$\frac{1}{2} \mathbf{I}_p^{\mathrm{H}} \mathbf{Z}_0 \mathbf{I}_q = \left(1 + \mathrm{j}\lambda_p\right) \delta_{pq}. \tag{13}$$

Physical units of impedance matrix $\mathbf{Z}_0$ are $[\Omega\, \mathrm{m}^2]$.

Matrices $\mathbf{Z}_0^{\mathrm{m},k}$, $\mathbf{Z}_0^{\mathrm{m},0}$, $\mathbf{Z}_0^{\mathrm{e},k}$, and $\mathbf{Z}_0^{\mathrm{e},0}$ are made dimensionless.

[2] M. Capek, P. Hazdra, M. Masek, *et al.*, “Analytical representation of characteristic modes decomposition,” *IEEE Trans. Antennas Propag.*, vol. 65, no. 2, pp. 713–720, 2017. DOI: 10.1109/TAP.2016.2632725.

[3] Complex and Hermitian conjugate can be removed in case as the characteristic modes for PEC bodies are by definition real-valued.

The analytical differentiation of $\mathbf{Z}$ with respect to ω (normalized by ω) is

$$\omega \frac{\partial \mathbf{Z}_0}{\partial \omega} = \mathrm{j} Z_0 a^2 \left(ka \left(\mathbf{Z}_0^{\mathrm{m},k} + \mathbf{Z}_0^{\mathrm{m},0} - \mathrm{j} ka \mathbf{T}^{\mathrm{m}} \right) + \frac{1}{ka} \left(\mathbf{Z}_0^{\mathrm{e},k} + \mathbf{Z}_0^{\mathrm{e},0} + \mathrm{j} ka \mathbf{T}^{\mathrm{e}} \right) \right), \tag{14}$$

where individual elements of the defining matrices are

$$T_{mn}^{\mathrm{m}} = \frac{1}{a^4} \int\limits_{\Omega} \int\limits_{\Omega} \boldsymbol{\psi}_m (\boldsymbol{r}) \cdot \boldsymbol{\psi}_n (\boldsymbol{r}') \frac{\mathrm{e}^{-\mathrm{j}kR}}{4\pi} \,\mathrm{d}S \,\mathrm{d}S', \tag{15}$$

$$T_{mn}^{\mathrm{e}} = \frac{1}{a^2} \int\limits_{\Omega} \int\limits_{\Omega} \nabla \cdot \boldsymbol{\psi}_m (\boldsymbol{r}) \,\nabla' \cdot \boldsymbol{\psi}_n (\boldsymbol{r}') \frac{\mathrm{e}^{-\mathrm{j}kR}}{4\pi} \,\mathrm{d}S \,\mathrm{d}S', \tag{16}$$

and

$$R = \left| \boldsymbol{r} - \boldsymbol{r}' \right|, \quad a = \max_{\boldsymbol{r}, \boldsymbol{r}' \in \Omega} \left\{ \frac{R}{2} \right\}, \quad Z_0 = \sqrt{\frac{\mu_0}{\varepsilon_0}}. \tag{17}$$

The stored energy matrix[4] for $ka < 1$ is defined as

$$\mathbf{W} = \operatorname{Im}\left\{\omega \frac{\partial \mathbf{Z}_0}{\partial \omega}\right\}. \tag{18}$$

and the stored electric and magnetic energies are

$$\mathbf{X}_\mathrm{m} = \frac{1}{2}\left(\mathbf{W} + \mathbf{X}_0\right), \tag{19}$$

$$\mathbf{X}_\mathrm{e} = \frac{1}{2}\left(\mathbf{W} - \mathbf{X}_0\right). \tag{20}$$

Therefore, the following identities holds

$$\mathbf{X}_0 = \mathbf{X}_\mathrm{m} - \mathbf{X}_\mathrm{e}, \tag{21}$$

$$\mathbf{W} = \mathbf{X}_\mathrm{m} + \mathbf{X}_\mathrm{e}. \tag{22}$$

[4] R. F. Harrington and J. R. Mautz, "Control of radar scattering by reactive loading," *IEEE Trans. Antennas Propag.*, vol. 20, no. 4, pp. 446–454, 1972. DOI: 10.1109/TAP.1972.1140234.

The basis function overlapping matrix $\mathbf{\Psi} = [\Psi_{mn}] \in \mathbb{R}^{N \times N}$ is defined element-wise as[5]

$$\Psi_{mn} = \int\limits_{\Omega} \boldsymbol{\psi}_m(\boldsymbol{r}) \cdot \boldsymbol{\psi}_n(\boldsymbol{r}) \, \mathrm{d}S. \tag{23}$$

The charge accumulation matrix $\mathbf{Q} = [Q_{mn}] \in \mathbb{R}^{N \times N}$ is defined element-wise as

$$Q_{mn} = \int\limits_{\Omega} \nabla \cdot \boldsymbol{\psi}_m(\boldsymbol{r}) \, \nabla \cdot \boldsymbol{\psi}_n(\boldsymbol{r}) \, \mathrm{d}S. \tag{24}$$

Properties of matrices $\mathbf{\Psi}$ and $\mathbf{Q}$:

- all eigenvalues are strictly positive (non-negative),
- they are sparse Gram matrices,
- elements Ψ_{mn} of $\mathbf{\Psi}$ might be zero even for overlapping basis functions.

[5] L. Jelinek and M. Capek, "Optimal currents on arbitrarily shaped surfaces," *IEEE Trans. Antennas Propag.*, vol. 65, no. 1, pp. 329–341, 2017. DOI: 10.1109/TAP.2016.2624735.

Lossy Matrix

The dissipation (ohmic) losses matrix $\mathbf{R}_\rho = [R_{\rho,mn}] \in \mathbb{R}^{N\times N}$ as

$$R_{\rho,mn} = \int\limits_{\Omega} R_\mathrm{s}\left(\boldsymbol{r}\right) \boldsymbol{\psi}_m\left(\boldsymbol{r}\right) \cdot \boldsymbol{\psi}_n\left(\boldsymbol{r}\right) \, \mathrm{d}S, \tag{25}$$

with $R_\mathrm{s}\left(\boldsymbol{r}\right) \geq 0$ being spatially dependent surface resistivity. For $R_\mathrm{s}\left(\boldsymbol{r}\right) = R_\mathrm{s}$

$$\mathbf{R}_\rho = R_\mathrm{s} \mathbf{\Psi}. \tag{26}$$

- There is charge density accumulated along a boundary of material inhomogeneity.

Impedance Matrix with Losses and Reactive Elements

The dissipation loss matrix $\mathbf{R}_\rho$ and matrix of lumped elements $\mathbf{Z}_\mathrm{L} = [Z_{\mathrm{L},mn}]$ can be added to the impedance matrix as

$$\mathbf{Z} = \mathbf{R}_\rho + \mathbf{Z}_0 + \mathbf{Z}_\mathrm{L}. \tag{27}$$

The lumped element matrix elements read

$$Z_{\mathrm{L},nn} = l_n^2 \left(R_n + \mathrm{j} \left(\omega L_n - \frac{1}{\omega C_n} \right) \right). \tag{28}$$

Excitation vector $\mathbf{V}$ defined element-wise:

$$V_n = \int\limits_{\Omega} \boldsymbol{\psi}_n \left(\boldsymbol{r}\right) \cdot \boldsymbol{E}_{\mathrm{i}} \left(\boldsymbol{r}\right) \, \mathrm{d}S. \tag{29}$$

Normalization matrix which deduces $[\Omega \, \mathrm{m}^2]$ dimensions to $[\Omega]$ is

$$D_n = l_n, \tag{30}$$

where l_n is length of the n-th basis function (see the introductory figure).

The matrix $\mathbf{D}$ is applied as

$$\widetilde{\mathbf{A}} = \mathbf{D}^{-\mathrm{T}} \mathbf{A} \mathbf{D}^{-1}. \tag{31}$$

Matrix $\mathbf{C} \in \{0,1\}^{N \times P}$ mapping selected edge(s)/port(s) onto the structure is defined as

$$C_{np} = \begin{cases} 1 & p\text{-th port is placed at } n\text{-th position}, \\ 0 & \text{otherwise}, \end{cases} \tag{32}$$

Port quantities are defined through controllable voltages $\mathbf{v}$ of dimensions [V]

$$\mathbf{V} = \mathbf{DCv}. \tag{33}$$

All quadratic-based observables are preserved, *i.e.*,

$$\mathbf{I}^{\mathrm{H}} \mathbf{A} \mathbf{I} = \mathbf{v}^{\mathrm{H}} \mathbf{a}^{\mathrm{H}} \mathbf{v}, \tag{34}$$

where

$$\mathbf{a} = \mathbf{C}^{\mathrm{H}} \mathbf{D}^{\mathrm{H}} \mathbf{Y}^{\mathrm{H}} \mathbf{AYDC} \in \mathbb{C}^{P \times P} \tag{35}$$

is port-representation of matrix $\mathbf{A}$.

The far-field is defined as

$$F(\hat{\boldsymbol{r}}, \hat{\boldsymbol{e}}) = \lim_{r \to \infty} \left\{ r \mathrm{e}^{\mathrm{j} k r} \hat{\boldsymbol{e}} \cdot \boldsymbol{E}(\boldsymbol{r}) \right\}. \tag{36}$$

Explicitly,

$$F(\hat{\boldsymbol{r}}, \hat{\boldsymbol{e}}) = -\frac{\mathrm{j} Z_0 k}{4\pi} \int\limits_{\Omega} \hat{\boldsymbol{e}} \cdot \boldsymbol{J}(\boldsymbol{r}') \, \mathrm{e}^{\mathrm{j} k \hat{\boldsymbol{r}} \cdot \boldsymbol{r}'} \, \mathrm{d}S, \tag{37}$$

and

$$U(\hat{\boldsymbol{r}}, \hat{\boldsymbol{e}}) = \frac{1}{2 Z_0} \left| F(\hat{\boldsymbol{r}}, \hat{\boldsymbol{e}}) \right|^2, \quad U(\hat{\boldsymbol{r}}) = U(\hat{\boldsymbol{r}}, \hat{\boldsymbol{\varphi}}) + U\left(\hat{\boldsymbol{r}}, \hat{\boldsymbol{\vartheta}}\right), \tag{38}$$

$$P_{\mathrm{rad}} = \int\limits_{S^2} U(\hat{\boldsymbol{r}}) \, \mathrm{d}S, \quad D(\hat{\boldsymbol{r}}, \hat{\boldsymbol{e}}) = \frac{4\pi U(\hat{\boldsymbol{r}}, \hat{\boldsymbol{e}})}{P_{\mathrm{rad}}}. \tag{39}$$

Radiation intensity matrix $\mathbf{U} = [U_{mn}]$ for direction $\hat{\boldsymbol{r}}$ and polarization $\hat{\boldsymbol{e}}$ is defined[6] as

$$U_{mn}(\hat{\boldsymbol{r}}, \hat{\boldsymbol{e}}) = \frac{Z_0 k^2}{32\pi^2} \int\limits_{\Omega} \int\limits_{\Omega} (\hat{\boldsymbol{e}} \cdot \boldsymbol{\psi}_m)(\hat{\boldsymbol{e}} \cdot \boldsymbol{\psi}_n)\, \mathrm{e}^{-\mathrm{j}k\hat{\boldsymbol{r}}\cdot(\boldsymbol{r}-\boldsymbol{r}')}\, \mathrm{d}S\, \mathrm{d}S', \tag{40}$$

and it is a rank-one matrix as the far-field vector $\mathbf{F} = [F_n]$ defined as

$$F_n(\hat{\boldsymbol{r}}, \hat{\boldsymbol{e}}) = \frac{-\mathrm{j}Z_0 k}{4\pi} \int\limits_{\Omega} \hat{\boldsymbol{e}} \cdot \boldsymbol{\psi}_n \mathrm{e}^{\mathrm{j}k\hat{\boldsymbol{r}}\cdot\boldsymbol{r}}\, \mathrm{d}S \tag{41}$$

can be used

$$\mathbf{U}(\hat{\boldsymbol{r}}, \hat{\boldsymbol{e}}) = \frac{1}{2Z_0}\mathbf{F}(\hat{\boldsymbol{r}}, \hat{\boldsymbol{e}})\,\mathbf{F}^{\mathrm{H}}(\hat{\boldsymbol{r}}, \hat{\boldsymbol{e}}). \tag{42}$$

Total radiation intensity can be calculated as

$$\mathbf{U}(\hat{\boldsymbol{r}}) = \mathbf{U}(\hat{\boldsymbol{r}}, \hat{\boldsymbol{\varphi}}) + \mathbf{U}\left(\hat{\boldsymbol{r}}, \hat{\boldsymbol{\vartheta}}\right). \tag{43}$$

[6] L. Jelinek and M. Capek, "Optimal currents on arbitrarily shaped surfaces," *IEEE Trans. Antennas Propag.*, vol. 65, no. 1, pp. 329–341, 2017. DOI: 10.1109/TAP.2016.2624735.

Spherical waves can be projected onto basis functions as[7]

$$S_{t,\alpha n} = k\sqrt{Z_0} \int\limits_{\Omega} \mathbf{u}_{\alpha}^{(t)}\left(k\boldsymbol{r}\right) \cdot \boldsymbol{\psi}_n\left(\boldsymbol{r}\right) \,\mathrm{d}S, \tag{44}$$

α is multi-index accommodating σ, m, l, and $\mathbf{u}_{\alpha}^{(t)}\left(k\boldsymbol{r}\right)$ are the spherical waves of proper type[8].

We have four types of matrix $\mathbf{S}_t$, $t \in \{1, \dots, 4\}$. They are capable of various projections.

Matrix $\mathbf{S}_t \in \mathbb{R}^{N_\alpha \times N}$ is a projection matrix between RWG basis and spherical waves basis. It is low-rank matrix in α, suitable for compression techniques.

[7] D. Tayli, M. Capek, L. Akrou, *et al.*, "Accurate and efficient evaluation of characteristic modes," *IEEE Trans. Antennas Propag.*, vol. 66, no. 12, pp. 7066–7075, 2018. DOI: 10.1109/TAP.2018.2869642.

[8] G. Kristensson, *Scattering of Electromagnetic Waves by Obstacles*. Edison, NJ: SciTech Publishing, an imprint of the IET, 2016.

Relation Between Radiation Matrix and Spherical Waves Matrix

The relationship between resistance part of impedance matrix and spherical waves matrix

$$\mathbf{R}_0 = \mathbf{S}_1^{\mathrm{T}} \mathbf{S}_1. \tag{45}$$

- Resulting radiation matrix has no negative eigenvalues (many of them are zero, however).
- The number of spherical waves to be used

$$N_\alpha = 2 l_{\max} \left(l_{\max} + 2 \right), \tag{46}$$

$$l_{\max} = \lceil 3 + ka + 7 \sqrt[3]{ka} \rceil. \tag{47}$$

For Ω being a spherical shell, the rows of matrix $\mathbf{S}_t$ contains directly the expansion coefficients of corresponding spherical waves, $\mathbf{I}_\alpha$, since

$$\mathbf{I}_{\alpha p}^{\mathrm{H}} \mathbf{S}_t^{\mathrm{H}} \mathbf{S}_t \mathbf{I}_{\alpha q} = \left| \mathbf{S}_t \mathbf{I}_{\alpha p} \right|^2 \delta_{pq} = \left| f_{t,\alpha p} \right|^2 \delta_{pq} = K_{t,\alpha} \delta_{pq}, \tag{48}$$

where K_α is arbitrary constant depending on scaling.

Scattering T-matrix is defined as

$$\mathbf{T} = -\mathbf{S}_1 \mathbf{Z}^{-1} \mathbf{S}_1^{\mathrm{T}}. \tag{49}$$

Then, *e.g.*, the characteristic modes defined in spherical mode basis are

$$\mathbf{T}\mathbf{f}_{1,p} = -\frac{1}{1 + \mathrm{j}\lambda_p} \mathbf{f}_{1,p} \tag{50}$$

with $\mathbf{f}_{1,p} = -\mathbf{S}_1 \mathbf{I}_p$.

- The eigenvalue problem is reduced from generalized to standard one.
- The numerical precision increases from double to octuple precision.
- The problem is reduced in size by removing zero rows from $\mathbf{S}_1$ matrix.

The radiated far-field can be expressed as

$$\boldsymbol{F}\left(\hat{\boldsymbol{r}}\right) = \frac{1}{k} \sum_{\alpha} \mathrm{j}^{l-\tau+2} f_\alpha \mathbf{Y}_\alpha\left(\hat{\boldsymbol{r}}\right), \tag{51}$$

where $\mathbf{Y}_\alpha\left(\hat{\boldsymbol{r}}\right)$ are the real-valued spherical vector harmonics and

$$\left[f_\alpha\right] = \mathbf{S}_1 \mathbf{I}, \quad f_\alpha \in \mathbb{R}^{1\times 1}. \tag{52}$$

Then we get a series of equalities

$$P_{\mathrm{rad}} \approx \frac{1}{2} \mathbf{I}^{\mathrm{H}} \mathbf{R}_0 \mathbf{I} = \frac{1}{2} \left|\mathbf{S}_1 \mathbf{I}\right|^2 = \frac{1}{2} \sum_{\alpha} \left|f_\alpha\right|^2 = \mathbf{I}^{\mathrm{H}} \int\limits_{S^2} \Big(\mathbf{U}\left(\hat{\boldsymbol{r}}, \hat{\boldsymbol{\varphi}}\right) + \mathbf{U}(\hat{\boldsymbol{r}}, \hat{\boldsymbol{\vartheta}})\Big) \,\mathrm{d}S\, \mathbf{I}, \tag{53}$$

with S^2 being unit sphere.

Electric and magnetic fields are approximated as

$$\boldsymbol{N}_{\mathrm{e},n}(\boldsymbol{r}) = -\mathrm{j}Z_0k^2 \int\limits_{\Omega} \left((\hat{\boldsymbol{r}} \times \boldsymbol{\psi}_n) \times \hat{\boldsymbol{r}} + (3\hat{\boldsymbol{r}}(\hat{\boldsymbol{r}} \cdot \boldsymbol{\psi}_n) - \boldsymbol{\psi}_n) \left(\frac{1}{(kR)^2} + \frac{\mathrm{j}}{kR} \right) \right) \frac{\mathrm{e}^{-\mathrm{j}kR}}{4\pi kR} \, \mathrm{d}S, \tag{54}$$

$$\boldsymbol{N}_{\mathrm{m},n}(\boldsymbol{r}) = -\mathrm{j}k^2 \int\limits_{\Omega} (\hat{\boldsymbol{r}} \times \boldsymbol{\psi}_n) \left(1 + \frac{1}{\mathrm{j}kR} \right) \frac{\mathrm{e}^{-\mathrm{j}kR}}{4\pi kR} \, \mathrm{d}S. \tag{55}$$

with $\mathbf{N}_\mathrm{e} = [\boldsymbol{N}_{\mathrm{e},n}], \mathbf{N}_\mathrm{m} = [\boldsymbol{N}_{\mathrm{m},n}] \in \mathbb{C}^{N \times 3}$.

Notice then that

$$\boldsymbol{E}(\boldsymbol{r}) \approx \mathbf{N}_\mathrm{e}(\boldsymbol{r})\,\mathbf{I}, \tag{56}$$

$$\boldsymbol{H}(\boldsymbol{r}) \approx \mathbf{N}_\mathrm{m}(\boldsymbol{r})\,\mathbf{I}. \tag{57}$$

Electric dipole moment matrix $\mathbf{p} = [\boldsymbol{p}_n] \in \mathbb{R}^{N\times 3}$ is defined as

$$\boldsymbol{p}_n = \frac{\mathrm{j}}{\omega} \int\limits_{\Omega} \boldsymbol{r} \nabla \cdot \boldsymbol{\psi}_n \, \mathrm{d}S = \frac{1}{\mathrm{j}\omega} \int\limits_{\Omega} \boldsymbol{\psi}_n \, \mathrm{d}S. \tag{58}$$

Magnetic dipole moment matrix $\mathbf{m} = [\boldsymbol{m}_n] \in \mathbb{R}^{N\times 3}$ is defined as

$$\boldsymbol{m}_n = \frac{1}{2} \int\limits_{\Omega} \boldsymbol{r} \times \boldsymbol{\psi}_n \, \mathrm{d}S \tag{59}$$

Squared magnitude of the electric and magnetic dipole moments can be calculated as

$$|\boldsymbol{p}|^2 = \mathbf{I}^{\mathrm{H}} \mathbf{P} \mathbf{I}, \tag{60}$$

$$|\boldsymbol{m}|^2 = \mathbf{I}^{\mathrm{H}} \mathbf{M} \mathbf{I}, \tag{61}$$

where matrices $\mathbf{P} \in \mathbb{R}^{N\times N}$ and $\mathbf{M} \in \mathbb{R}^{N\times N}$ are

$$\mathbf{P} = \mathbf{p}\mathbf{p}^{\mathrm{H}}, \tag{62}$$

$$\mathbf{M} = \mathbf{m}\mathbf{m}^{\mathrm{H}}. \tag{63}$$

$\mathcal{B}(\cdot)$ Boolean operator. All non-zero values are converted to logical true (1), all zero values are converted to logical false (0), *i.e.*, $\mathbf{A} = \mathcal{B}(\mathbf{Q})$ is equivalent to `A = logical(Q)` in MATLAB.

$\mathcal{R}(\cdot, r)$ Thresholding operator defined element-wise as

$$\mathcal{R}(x, r) = \begin{cases} 1 & \Leftrightarrow & x > r, \\ 0 & \Leftrightarrow & \text{otherwise.} \end{cases} \tag{64}$$

The following relation is valid irrespective of the inequality used for definition of $\mathcal{R}(\cdot, r)$ ($>$ vs. $\geq$)

$$\mathcal{B}(\mathbf{x}) = |\mathbf{1} - 2\mathcal{R}(\mathbf{x}, \mathbf{0})| \tag{65}$$

Adjacency Matrix

The adjacency matrix $\mathbf{A} = [A_{mn}] \in [0,1]^{N \times N}$ is defined as

$$A_{mn} = \begin{cases} 1 & \Leftrightarrow \quad \boldsymbol{\psi}_m(\boldsymbol{r}) \cup \boldsymbol{\psi}_n(\boldsymbol{r}) \neq 0, \\ 0 & \Leftrightarrow \quad \text{otherwise.} \end{cases} \tag{66}$$

The adjacency matrix in AToM is evaluated as “logical thresholding” of matrix $\mathbf{Q}$

$$\mathbf{A} = \mathcal{B}(\mathbf{Q}) . \tag{67}$$

Properties:

- sparsity for a sphere of T triangles with $N = 3T/2$ RWG basis functions is equal[9] to $1 - 5/N$.

[9] Topologically minimal S^2 sphere is a 3-simplex (tetrahedron), then $N = 6$ and each basis function $\boldsymbol{\psi}_n$ sees all the others except of one. All opened and simple structures have higher sparsity.

Mapping from set of basis functions into set of triangles is done via mapping (incidence) matrix $\mathbf{B} = [B_{tn}] \in [0,1]^{T \times N}$ which is defined element-wise as

$$B_{tn} = \begin{cases} 1 & \Leftrightarrow \quad \displaystyle\int\limits_{\triangle_t} \boldsymbol{\psi}_n(\boldsymbol{r}) \, \mathrm{d}S \neq 0, \\ 0 & \Leftrightarrow \quad \text{otherwise}, \end{cases} \tag{68}$$

where $\triangle_t$ is the region spanned by the t-th triangle.

There is relationship between adjacency and incidence matrix:

$$\mathbf{A} = \mathcal{B}\left(\mathbf{B}^{\mathrm{T}}\mathbf{B}\right). \tag{69}$$

Then, for example, the area occupied by an antenna represented by “genus” $\mathbf{g} \in \{0,1\}^{N \times 1}$ is

$$A = \mathbf{a}^{\mathrm{T}} \mathcal{B}\left(\mathbf{B}\mathbf{g}\right), \tag{70}$$

where $\mathbf{a} \in \mathbb{R}^{T \times 1}$ is the column vector containing areas of triangles.

Useful relations[10] are

$$\nabla \cdot \boldsymbol{\psi}_n \left(\boldsymbol{r}\right) = \pm \frac{l_n}{A_n^\pm}, \tag{71}$$

$$\int\limits_{\Omega} \boldsymbol{\psi}_n \left(\boldsymbol{r}\right) \, \mathrm{d}S = l_n \left(\boldsymbol{r}_n^{c+} - \boldsymbol{r}_n^{c-}\right), \tag{72}$$

$$\int\limits_{\Omega} \boldsymbol{r} \times \boldsymbol{\psi}_n \, \mathrm{d}S = \frac{l_n}{2} \left(\mathbf{P}_n^+ \times \boldsymbol{r}_n^{c+} - \mathbf{P}_n^- \times \boldsymbol{r}_n^{c-}\right), \tag{73}$$

$$\int\limits_{\Omega} \nabla \cdot \boldsymbol{\psi}_m \left(\boldsymbol{r}\right) \, \mathrm{d}S = \frac{l_n}{A_n^+} \int\limits_{A_n^+} \mathrm{d}S - \frac{l_n}{A_n^-} \int\limits_{A_n^-} \mathrm{d}S = 0, \tag{74}$$

where $\Omega = A_n^+ \cup A_n^-$.

[10] S. M. Rao, D. R. Wilton, and A. W. Glisson, "Electromagnetic scattering by surfaces of arbitrary shape," *IEEE Trans. Antennas Propag.*, vol. 30, no. 3, pp. 409–418, 1982. DOI: 10.1109/TAP.1982.1142818.

For $\boldsymbol{r} \equiv [x \; y \; z]$ the transformation from/to simplex coordinates (α, β, γ) reads

$$\boldsymbol{r} = \begin{bmatrix}\alpha & \beta & \gamma\end{bmatrix} \begin{bmatrix}\mathbf{P}_A \\ \mathbf{P}_B \\ \mathbf{P}^{\pm}\end{bmatrix}. \tag{75}$$

Notice that $\gamma = 1 - \alpha - \beta$, and

$$\int\limits_T f(\boldsymbol{r}) \, \mathrm{d}S = 2A \int\limits_0^1 \int\limits_0^{1-\alpha} f\left(\alpha \mathbf{P}_A + \beta \mathbf{P}_B + (1 - \alpha - \beta)\, \mathbf{P}^{\pm}\right) \mathrm{d}\beta \, \mathrm{d}\alpha. \tag{76}$$

Discretization grid and RWG basis functions:

Listing 1: atom_code1_mesh.m

```
% Frequency
f = atom.selectedProject.physics.getFrequencyListValues;
% or manually specified by user:
f = 1e9; % 1 GHz

% (It is expected that MoM requests are correctly set up.)
Res = atom.selectedProject.solver.MoM2D.results;

Mesh = Res.mesh;         % mesh grid
BF   = Res.basisFcns;    % basis functions

% Or without running MoM solver directly from AToM:
Mesh = atom.selectedProject.mesh.getMeshData2D();
BF   = models.solvers.MoM2D.basisFcns.getBasisFcns(Mesh);
```

Impedance matrix(-related) operators $\mathbf{Z}_0$, $\mathbf{W}$, $\mathbf{Z}_0^{M,k}$, $\mathbf{Z}_0^{M,0}$, $\mathbf{Z}_0^{E,k}$, $\mathbf{Z}_0^{E,0}$, $\mathbf{T}^M$, $\mathbf{T}^E$:

Listing 2: `atom_code1_MoM1.m`

```
% Impedance matrix
Z   = Res.zMat.data;

omega = 2*pi*f;
% Stored energy matrix
W   = omega*imag(Res.zMatD.data); % omega*DZ!

% Individual parts of impedance matrix:
ZMk  = Res.zMatMk.data;
ZM0  = Res.zMatM0.data;
ZEk  = Res.zMatEk.data;
ZE0  = Res.zMatE0.data;
TE   = Res.tMatE.data;
TM   = Res.tMatM.data;
```

Alternatively, $\mathbf{Z}_0$ and $\mathbf{W}$ can be calculated directly from normalized blocks:

Listing 3: atom_code1_MoM2.m

```
% Circumscribing sphere
a  = models.utilities.meshPublic.getCircumsphere(Mesh.nodes);
% Wavenumber and electrical size
k  = models.utilities.converter.f0tok0(f);
ka = k*a;

% Normalization constant
C  = a^2*Z0;

% Impedance matrix and stored energy matrix
Z  = 1j*C*(ka*(ZMk + ZM0) - 1/ka*(ZEk + ZE0));
W  = imag(1j*C*(ka*(ZMk + ZM0 - 1j*ka*TM) + 1/ka*(ZEk + ZE0 + 1j*ka*TE)));
```

Basis-function overlap matrix $\mathbf{\Psi}$ and related matrices $\mathbf{R}_\rho$, $\mathbf{A}$, and $\mathbf{B}$:

Listing 4: `atom_code1_LossyMatrix.m`

```
% The basis-function overlap matrix
Psi = models.utilities.matrixOperators.MoM2D.ohmicLosses.lossyMatrix(Mesh, BF);

% Dissipation losses matrix
Romega = Rs*Psi;

% RWG adjacency matrix
[A, T, F] = models.utilities.matrixOperators.MoM2D.divBasisFunctions. ...
    computeDivRhoDivRho(Mesh, BF);
A = sparse(logical(A));

% Basis functions to triangles matrix
BF2T = sparse(T.M + T.P).';

% Area spanned by genus g
gene = rand(BF.nUnknowns, 1) < 1/2;
Area = sum(Mesh.triangleAreas(logical(BF2T*gene)))
```

Far-field vectors **F** and matrix **U**:

Listing 5: atom_code1_farfield.m

```
% Theta and phi used to specify $\widehat{\boldsymbol{r}}$
theta = pi/2; % from 0 to pi
phi   = 0;    % from 0 to 2*pi
% Component used to specify $\widehat{\boldsymbol{e}}$
component = 'theta'; % component = {'theta' | 'phi' | 'total'}

% Far-field matrix (U) and vectors (F)
[U, F_phi, F_theta] = ...
    models.utilities.matrixOperators.MoM2D.farfield.computeU...
    (Mesh, BF, f, theta, phi, component)
```

Spherical wave projection matrix $\mathbf{S}_1$:

Listing 6: atom_code1_sphericalwaves.m

```
nQuad = 1;   % order of quadrature rule
Lmax  = 15; % highest degree of used Legendre polynomial

% Spherical wave projection matrix of size NxM
% N — number of spherical waves, M — number of RWG functions
S = models.utilities.matrixOperators.MoM2D.SMatrix.computeS...
    (Mesh, BF, f, Lmax, nQuad, 1);
```

Electric and magnetic dipole matrices $\mathbf{P}$ and $\mathbf{M}$, and vectors $\mathbf{p}$ and $\mathbf{m}$:

Listing 7: atom_code1_elmagMoments.m

```
% Electric moment matrix (P) and vector (p)
[P, p] = models.utilities.matrixOperators.MoM2D.electricMoment.computeP...
    (Mesh, BF, f);

% Magnetic moment matrix (M) and vector (m)
[M, m] = models.utilities.matrixOperators.MoM2D.magneticMoment.computeM...
    (Mesh, BF, f);
```

All operators can be gathered via standalone evaluation

Listing 8: atom_code1_evaluate_operators.m

```
% Zs is surface resistivity
Zs = 0.01; % copper at 1GHz
OP = models.utilities.matrixOperators.MoM2D.batch.evaluate(...
    Mesh, f, Zs, ...
    'requests', {'Z0', 'Xm', 'Xe', 'Rmat'}, 'quadOrder', 2, ...
    'useGPU', true);
% For the complete list of 'requests' see
models.utilities.matrixOperators.batch.getList
```

Far-field approximation

$$\boldsymbol{E}_{\mathrm{far}}\left(\boldsymbol{r}\right) = -\mathrm{j}\omega \boldsymbol{A}\left(\boldsymbol{r}\right), \quad \boldsymbol{A}\left(\boldsymbol{r}\right) = \frac{\mu_0}{4\pi} \int\limits_{\Omega} \boldsymbol{J}\left(\boldsymbol{r}'\right) \frac{\mathrm{e}^{-\mathrm{j}k\left|\boldsymbol{r}-\boldsymbol{r}'\right|}}{\left|\boldsymbol{r}-\boldsymbol{r}'\right|} \,\mathrm{d}S, \tag{77}$$

$$\text{with amplitude} \quad R \approx \left|\boldsymbol{r}\right| = r \quad \text{and phase} \quad R \approx r - \hat{\boldsymbol{r}} \cdot \boldsymbol{r}' \tag{78}$$

leads to

$$\boldsymbol{E}_{\mathrm{far}}\left(\boldsymbol{r}\right) = -\frac{\mathrm{j}Z_0 k}{4\pi} \frac{\mathrm{e}^{-\mathrm{j}kr}}{r} \int\limits_{\Omega} \boldsymbol{J}\left(\boldsymbol{r}'\right) \mathrm{e}^{\mathrm{j}k\hat{\boldsymbol{r}}\cdot\boldsymbol{r}'} \,\mathrm{d}S. \tag{79}$$

Questions?

For a complete PDF presentation see capek.elmag.org

Miloslav Čapek
miloslav.capek@antennatoolbox.com

May 24, 2021